INTERNATIONAL JOURNAL OF INTEGRATED ENGINEERING
ISSN: 2229-838X e-ISSN: 2600-7916

IJIE

Vol. 16 No. 2 (2024) 325-333
https://publisher.uthm.edu.my/ojs/index.php/ijie

Effect of Heating Power on The Synthesis of Titanium Dioxide Particles by Direct Heating Method for Photodegradation of Methylene Blue Solution

Chee Meng Koe[1], Guan Sheng Ng[1], Swee-Yong Pung[1]*

[1] *School of Materials and Mineral Resources Engineering, Engineering Campus, Universiti Sains Malaysia, 14300 Nibong Tebal, Pulau Pinang, MALAYSIA*

*Corresponding Author: sypung@usm.my
DOI: https://doi.org/10.30880/ijie.2024.16.02.033

Article Info

Received: 10 December 2023
Accepted: 15 June 2024
Available online: 17 August 2024

Keywords

Direct heating, photocatalyst, titanium dioxide

Abstract

Dyes are extensively used in the textile industry. Untreated dye-containing wastewater is hazardous to humans and the environment. Advanced oxidation processes (AOPs) based on heterogeneous TiO_2 photocatalyst is a technology that has been proven successful for effluent treatment. Nevertheless, use of TiO_2 photocatalyst in particles form could result in loss of TiO_2 photocatalyst over time during effluent treatment. Immobilization of TiO_2 photocatalyst on substrates could address this problem. In this study, a method called direct heating (DH) was devised to deposit TiO_2 particles on kanthal wires to prevent the particles from being washed away during effluent treatment. This method has low equipment cost and short synthesis duration when compared to others. The TiO_2 particles synthesized at 50 W in 15 min gave the best photodegradation efficiency, which was 36.3 % under 90 mins of UV light irradiation. It contained a mixture of anatase (22.5 %) and brookite (77.5 %), with an average particle size of 139.34 ± 15.89 nm. The TiO_2 particles had high surface coverage on kanthal wire with little agglomeration. The current work presents a captivating and low-cost setup, providing easy control over synthesis conditions and scaling potential for immobilizing TiO_2 particles on the kanthal wires.

1. Introduction

One of the most harmful pollutants in the world is dye. In many industries, including textiles, rubber, paper, food, and plastics, dyes are widely used. These industries produce coloured effluents even in low concentration (ppm level). The ecosystem and aquatic life will be severely harmed if the untreated dye effluent is discharged into water systems. The textile industry is one of the biggest sources of dye effluent pollutants overall since dyeing requires a significant amount of water [1].

In most cases, AOPs could degrade the organic pollutants in wastewater with powerful oxidants, i.e., hydroxyl radicals [2]. The non-biodegradable and extremely stable organic molecules could be broken down using AOP based on semiconductor photocatalysts. Due to the presence of electron-hole pairs, the presence of catalyst will speed up the AOPs. Free radicals were created by the photogenerated electrons and holes, which effectively oxidized and reduced the organic contaminants [3]. Upon completion of the photocatalytic process, the organic pollutants will disintegrate into smaller molecules like water and carbon dioxide. TiO_2 is a popular photocatalyst for the removal of organic dyes [4, 5]. The use of TiO_2 photocatalyst in particle form is not suitable as it tends to drain away in wastewater. To lessen the gradual loss of TiO_2 photocatalyst during effluent treatment, attempts have been made to grow TiO_2 photocatalyst on supporting substrates.

This is an open access article under the CC BY-NC-SA 4.0 license.

TiO_2 particles could be synthesized using a variety of synthetic methods, including hydrothermal method [6] template-assisted method [7], sol-gel method [8], electrochemical anodizing method [9], microwave-assisted method [10], and chemical vapour deposition method [11]. The main drawbacks of these approaches are either incurred of high equipment costs, high electrical power consumption, or lengthy synthesis times. For instance, Sun et al. [12] took 36 hrs to produce TiO_2 nanotubes using hydrothermal method; whereas Qiang Zhang et al. [13] synthesized TiO_2 films between 300 ℃ to 400 ℃ using chemical vapour deposition method. In these synthesis methods, heat is first created outside the reactor and then transferred into the reactor chamber. As a result, heat is squandered in large amounts across the area, causing long synthesis duration (in hours) and high electrical power consumption (in kW.h).

DH method is a simple, and one-step process for the synthesis of nanomaterials. In our earlier work, TiO_2 particles were synthesized using DH method [14]. We also demonstrated that the immobilization of ZnO rods and TiO_2 particles on kanthal wires using this method [15, 16]. **Table 1** summarises the estimated synthesis duration, equipment cost, and energy needed for common synthesis methods used to produce TiO_2. It could be seen that DH method takes less than 1 hour for the synthesis of TiO_2 nanoparticles (without immobilized on substrate) [15], whereas hydrothermal takes more than 61 hours, and sol-gel method takes more than 12 hours. Moreover, DH method only used RM 710 for equipment cost, which is cheaper than the hydrothermal method (RM 16789.45) and the sol-gel method (RM 19330.67). Moreover, DH method only uses 0.06 kWh per run, which leads to a (RM 0.01332) energy consumption cost per run. This is cheaper than hydrothermal method (RM 13.26672) and sol-gel method (RM 4.8063).

Table 1 *A comparison of synthesis duration, equipment cost, energy used and operational cost for the synthesis of TiO_2 particles*

Methods	Synthesis Duration (hour)	Equipment Cost (RM)	Energy used (kWh)	Energy Consumption Cost (RM)
Hydrothermal	> 61	16789.45	59.76	RM 13.2667
Sol-gel	> 12	19330.67	21.65	RM 4.8063
Direct Heating Method	< 1	710.00	0.06	RM 0.0133

In this work, the effect of heating power on the deposition of TiO_2 particles using DH method was investigated. The study showed that heating the kanthal wire with 50 W for 15 min was sufficient to deposit TiO_2 particles on kanthal wires with good surface coverage and photodegradation efficiency. The rapid synthesis process was achieved due to very little heat loss to the environment.

2. Materials and Methods

2.1 Deposition of TiO2 Particles on Kanthal Coils by DH Method

A 30 cm length of kanthal wire with a diameter of 0.812 mm was cut from the wire spool by a wire cutter. It was winded around a pen to produce a wire coil with 8 turns without overlapping. The coil was 20 mm in length. Under sonification, the kanthal coil was cleaned and degreased in an acetone bath for 15 min. After that, cleaning was done for 15 min while being sonicated in an isopropanol bath. The coil was then cleaned for a further 10 min in a deionized water bath before air dried.

Fig. 1 shows the setup of DH method. The precursor solution was prepared by mixing 5 ml of titanium tetraisopropoxide (TTIP) (Sigma Aldrich) with 15 ml of isopropanol (Sigma Aldrich). Separately, a 250 ml solution of distilled water was adjusted to pH 1 using hydrochloric acid (HCl) (QReC). To this acidic solution, 2 drops of hydrogen peroxide (H2O2) (Merck) were added as an oxidizing agent to facilitate the formation of TiO_2. The TTIP mixture was then hydrolysed by being added dropwise into the acidic solution while continuously stirring with a magnetic stirrer. Following this, the kanthal coil was immersed in the precursor solution, and the electrical power supply was turned on. The effect of heating power on the deposition of TiO_2 particles on the surface of kanthal wires was studied. The heating power was varied from 30, 40, and 50 W but the heating duration was fixed at 15 min. At the end of synthesis process, the kanthal coils were rinsed with distilled water and air dried prior to characterization. Fig. 2 (a) shows the schematic diagram of location where temperatures were measured with the Uni-T UT320D Digital Thermometer 2-Channel Type K/J. Point A was at kanthal coil, whereas Point B was at the position near to the bottom of beaker. Fig. 2(b) shows the schematic diagram of TiO_2 particles that were grown on kanthal wire and its by-product.

Int. Journal of Integrated Engineering Vol. 16 No. 2 (2024) p. 325-333

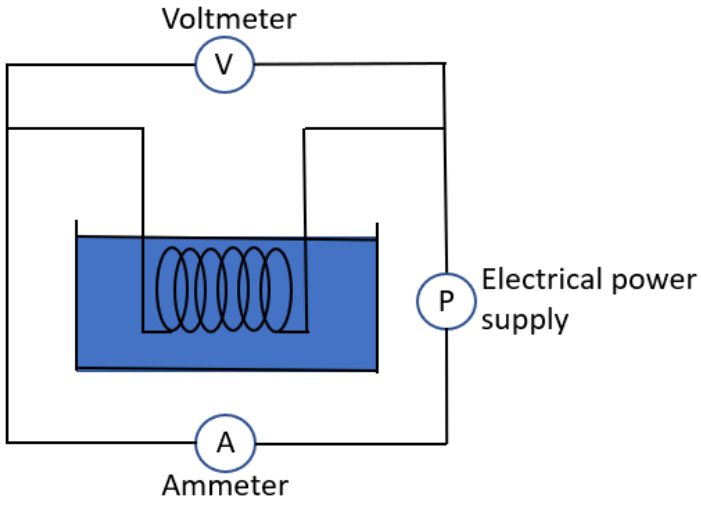

Fig. 1 *Schematic diagram of the setup of DH method*

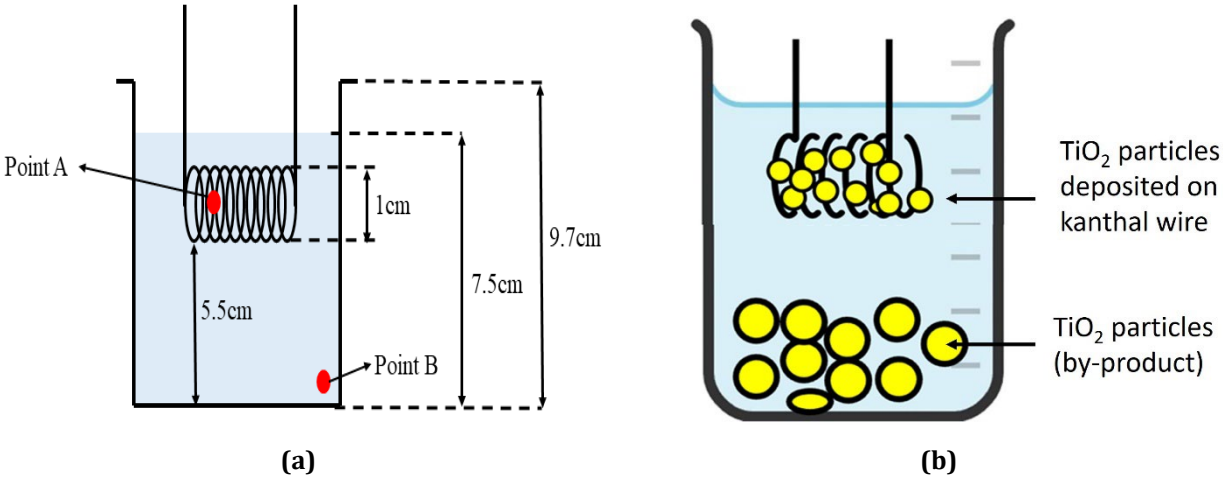

Fig. 2 *Schematic diagram of (a) Setup of DH method; (b) TiO_2 particles that were deposited on kanthal wire and its by-product (at the bottom of the beaker)*

The morphology of the deposit was characterized using a scanning electron microscope (FEI Quanta 650 FEG Scanning Electron Microscope). The size of the particles that deposited on the kanthal wire was subsequently measured by Image J software. The quantity of deposit found on the surface of kanthal coils was small. In addition, the bending of kanthal coils made it difficult to analyse for its structural and optical properties. Therefore, the deposits (by-product) at the bottom of the beaker were collected and dried prior to analysis. The crystal phases of deposits were characterized using an X-ray diffractometer (XRD, Bruker D2 Phaser). The XRD target was copper, emitting X-ray with a 0.15406 nm wavelength (Cu K_α). The scanning range of XRD analysis was performed from 10º to 90º of 2θ at an accelerating voltage of 30 kV. The XRD data was analysed by X'pert Highscore Plus software. The spectrum obtained from Fourier-transform infrared spectroscopy (FTIR, Perkin Elmer) was used to identify the functional groups of as-synthesized particles. The UV-visible spectrometer (Varian Cary 50) was used to measure the characteristic absorbance of degraded MB solution at 664 nm.

2.2 Photocatalytic Degradation of Methylene Blue Solution by TiO_2 Particles

The photocatalytic activity of the TiO_2 particles deposited on kanthal coils was studied. The coils with TiO_2 deposits and 100 ml of MB solution (1 mg L^{-1}) were kept in a beaker. To achieve adsorption-desorption between the MB solution and the surface of the TiO_2 particles, the solution was stirred in the dark for 30 min [17]. The photocatalytic process was then started by turning on the UV light (wavelength: 254 nm) at room temperature. 4.5 mL of aliquots were sampled every 15 min until 90 minutes. By using UV-Visible spectroscopy, the absorbance of the samples collected at various time intervals was measured. The concentration of MB proportional directly to

its absorbance intensity (λ = 664 nm) as stated in Beer-Lambert rule. The photodegradation efficiency of TiO_2 particles deposited on kanthal coils in the removal of MB could be calculated using Equation 1:

$$Photodegradation\ efficiency\ (\%) = \frac{C_0 - C_t}{C_0}\ x\ 100 = \frac{I_0 - I_t}{I}\ x\ 100 \quad (1)$$

where C_o is the initial MB concentration in the solution, C_t is the residual MB concentration, I_0 is the initial absorbance intensity, and I_t is the residual absorbance intensity after the irradiation time (t), respectively.

3. Results and Discussion

Fig. 3 shows the temperature profile at points A and B as a function of heating duration using various heating powers. In general, the temperature at Point A (near kanthal wire) rose rapidly as compared to Point B (at the bottom of beaker). The temperatures at Point B almost remained constant throughout the heating duration for all heating powers. It is also noted that higher heating power obtained higher heating rate, achieving higher temperature in shorter duration. For instance, it recorded 85 °C at 15 min when using 50 W heating power.

The morphology of TiO_2 particles that deposited on kanthal wires produced using various heating powers are shown in Fig. 4. Fig. 4 (a) depicts that no deposition was discovered on the surface of kanthal wire using 0 W of heating power. As shown in Fig. 4 (b) – (d), TiO_2 particles were deposited on the surface of kanthal wires at all heating powers. With the increase of heating power from 30 W to 50 W, the surface coverage of TiO_2 particles increases. This indicates that more TiO_2 particles were deposited on the surface of kanthal wires. A higher heating power resulted in a higher heating rate and a higher temperature on both the kanthal wire and precursor solution. This allowed more TiO_2 nucleation, and subsequently growth of TiO_2 particles on the surface of kanthal wire and in the precursor solution (by-product).

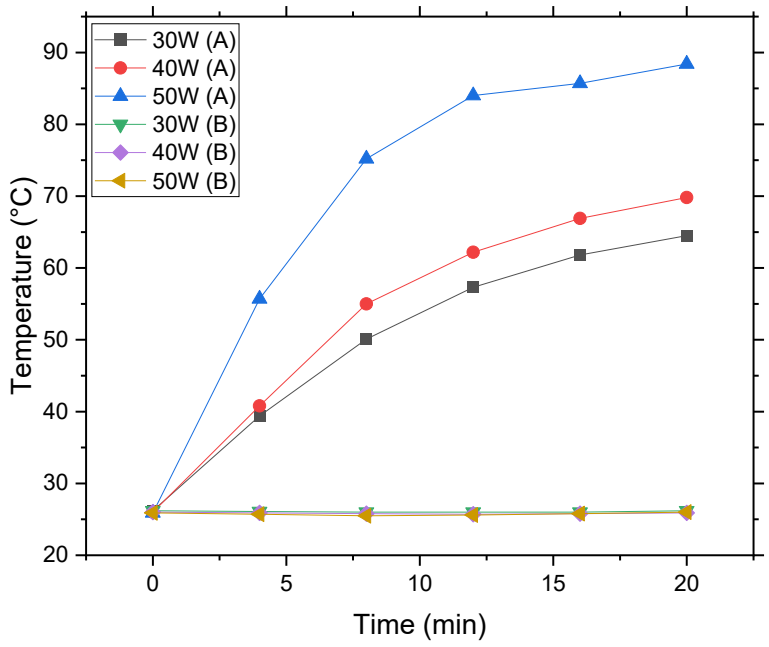

Fig. 3 *Temperature profile at point A and B against time*

Table 2 *The size of TiO_2 nanoparticles deposited on kanthal wires at various heating powers*

Heating power (W)	Diameter of TiO_2 nanoparticles (nm)	
	Mean	Standard Deviation
0	-	-
30	144.01	16.80
40	139.34	15.89
50	113.01	24.48

Int. Journal of Integrated Engineering Vol. 16 No. 2 (2024) p. 325-333

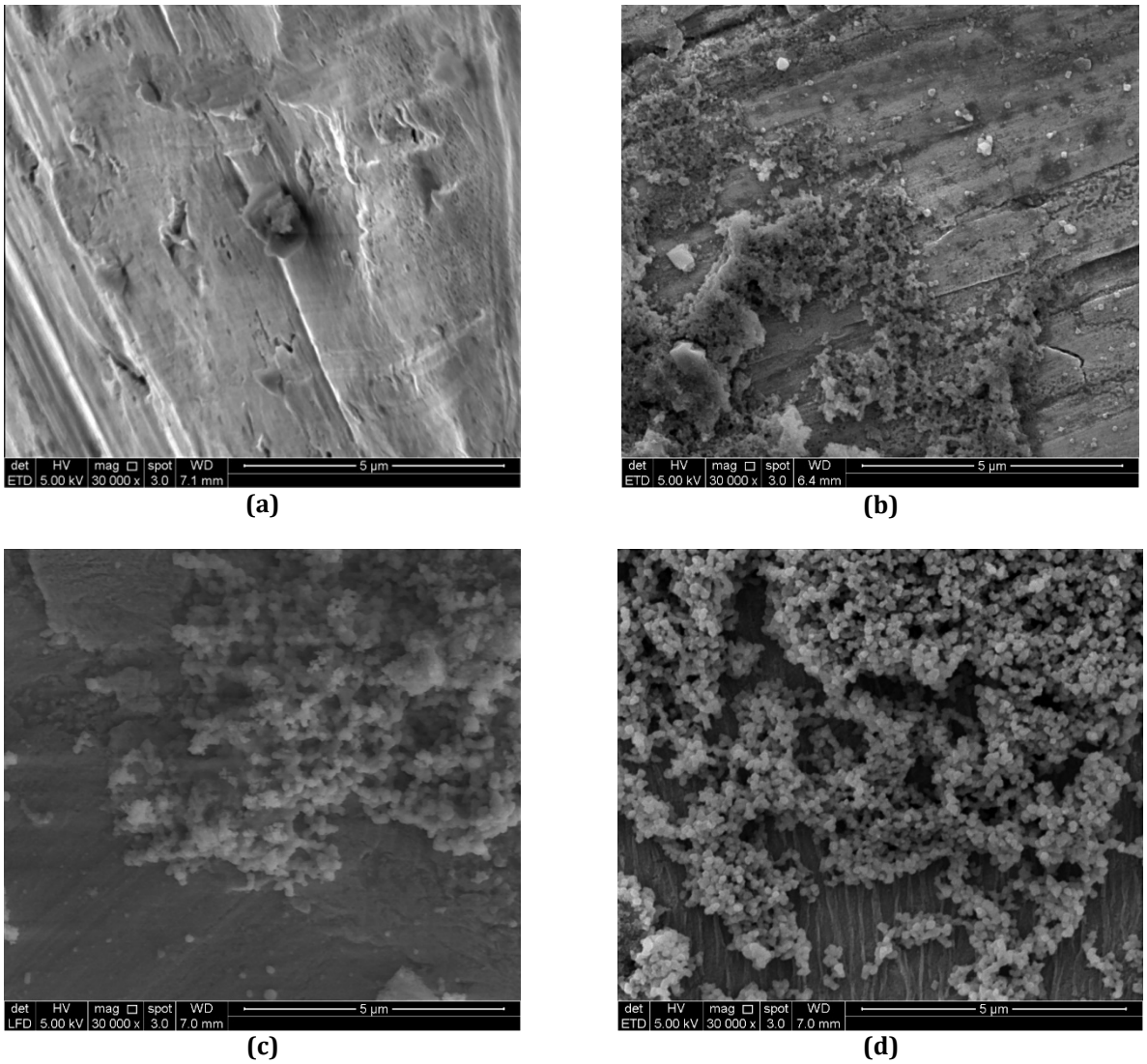

Fig. 4 *FESEM images of TiO_2 deposited on kanthal wires in pH 1 solution for 15 min at (a) 0, (b) 30, (c) 40, and (d) 50 W*

Table 3 *ANOVA table on particle size deposited using various heating powers*

Source	DF	Adj SS	Adj MS	F-Value	P-Value
Factor	2	16764	8382.1	22.18	0.000
Error	87	32881	377.9		
Total	89	49645			

The XRD patterns of particles (by-products) produced at various heating powers are displayed in Fig. 6. The diffraction peaks at the positions of 2θ = 25.28°, 37.60°, 48.00°, 53.92°, 69.00° could be indexed to the (101), (004), (200), (105), (116) of tetragonal anatase phase TiO_2 (ICSD 98-005-9309). It should be emphasised that all the particles produced by DH contained anatase TiO_2. Besides, the diffraction peaks at the positions of 2θ = 30.80°, 63.00° correspond to Miller indices of (121), (601) of an orthorhombic brookite TiO_2 (ICSD 98-010-5395). Anatase-phase crystallite is known to form earlier than o ther phases during the synthesis of TiO_2 particles. The amount of Anatase and Brookite produced by DH was estimated using the Rietveld refinement method. Based on the information presented in Table 4, the amount of anatase in the composition decreased while the amount of brookite increased as the heating power was raised (higher solution temperature). This observation is aligned with the finding of Tarek A. Kandiel et al [18]. According to their work, Anatase would change into brookite at temperature between < 600 °C attributed to the thermodynamic stability in these temperature range. In summary, the XRD results show that the DH method was successful in producing TiO_2 particles with a mixture of crystal phases, namely anatase and brookite.

The TiO_2 particles (by-products) produced by different heating powers were analysed by FTIR spectroscopy. Fig. 7 shows the FTIR spectrum of TiO_2 particles produced with different heating powers. The peak at 3376 cm^{-1} corresponds to both symmetric and asymmetric stretching vibrations of the hydroxyl group (OH group). The characteristic peak at 1633 cm^{-1} corresponds to the Ti-OH bending vibrations of the absorbed water molecules. Therefore, both peaks at 3376 cm^{-1} and 1633 cm^{-1} correspond to the surface adsorbed water and hydroxyl group. The presence of OH bands in the spectrum means the H_2O chemically and physically adsorbed on the surface of TiO_2 particles. In addition, the peak at 501 cm^{-1} is ascribed to the Ti-O stretching mode. It is noted that the peak in the range of 400 to 800 cm^{-1} represent the anatase TiO_2. However, the Ti-O peak is less intense, and it might be due to small crystallites size that result in the broadness of the peaks [17]. Therefore, both XRD and FTIR analyses indicate that the particles produced by DH were TiO_2, regardless of their heating power.

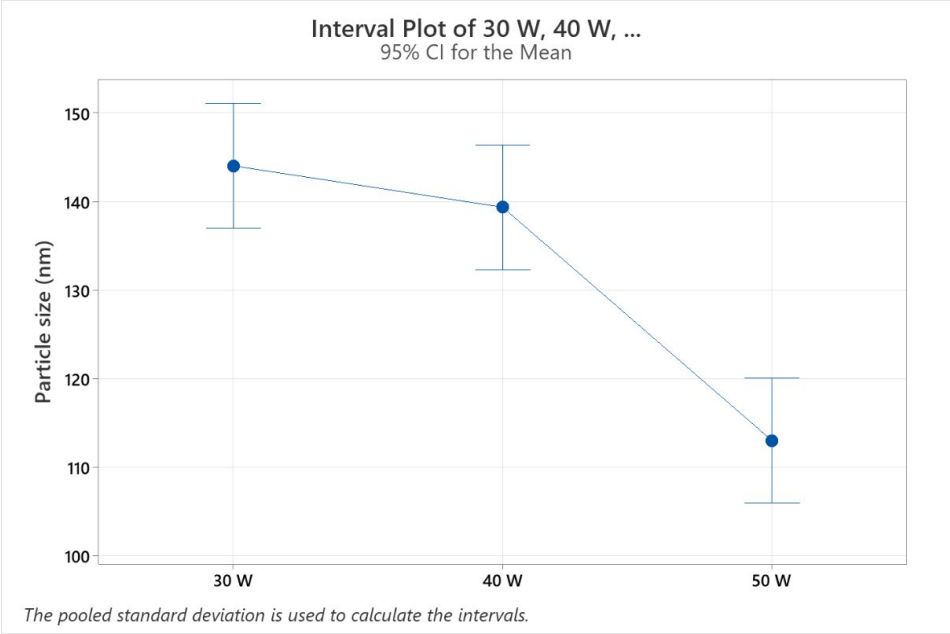

Fig. 5 *Interval plot of TiO_2 particles size deposited on kanthal wires by DH method using various heating power*

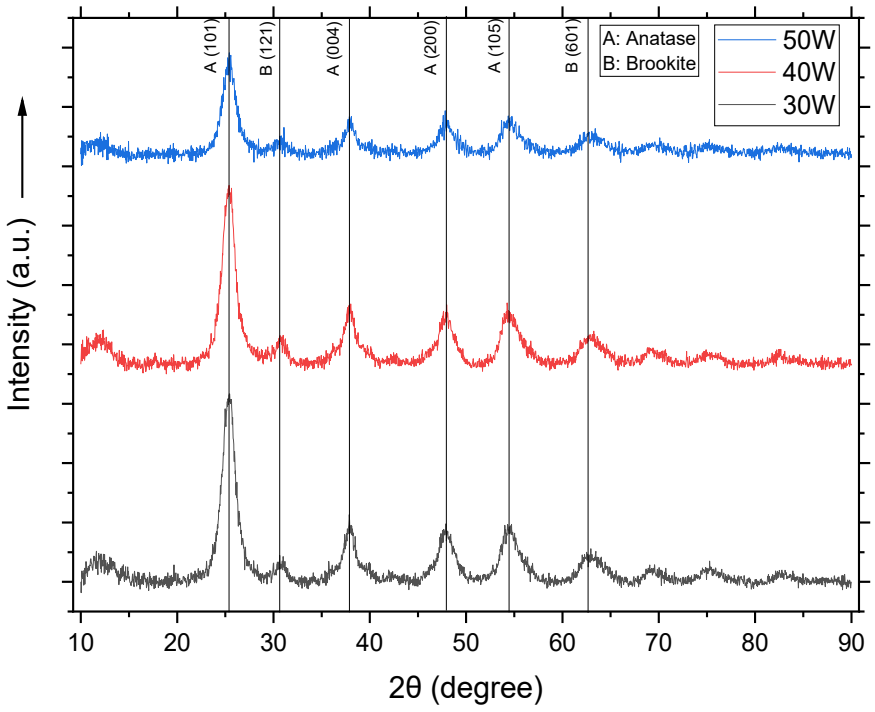

Fig. 6 *XRD patterns of TiO_2 particles produced by DH method using various heating powers*

Int. Journal of Integrated Engineering Vol. 16 No. 2 (2024) p. 325-333

Table 4 *The crystal phase content of TiO_2 particles produced by DH method using various heating powers*

Heating power (W)	Phase content (wt. %)	
	Anatase	Brookite
0	-	-
30	77.1	22.9
40	40.9	59.1
50	22.5	77.5

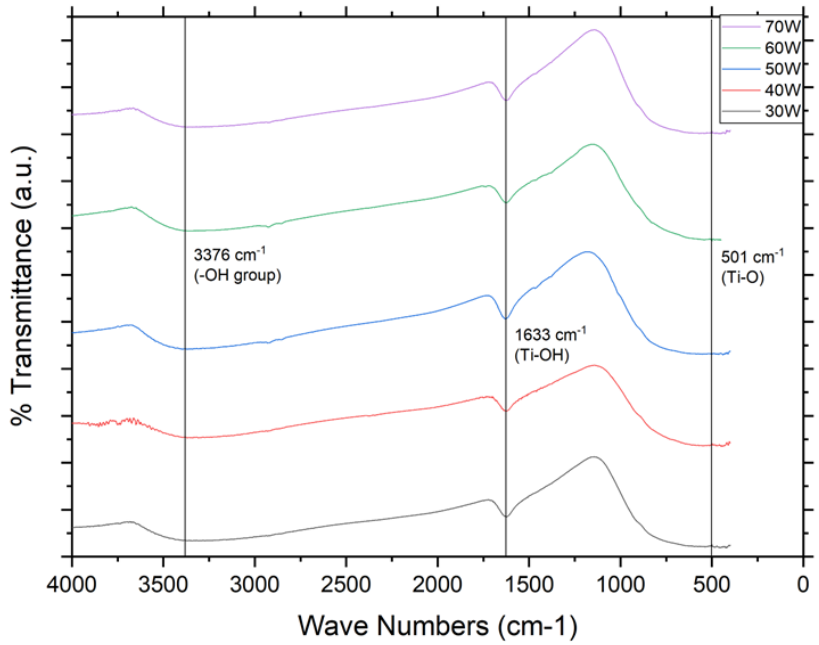

Fig. 7 *FTIR spectrum of TiO_2 particles (by-product) produced by DH method using various heating powers*

Fig. 8 displays the photodegradation efficiency of TiO_2 particles deposited on kanthal wires using various heating powers for 90 minutes. The lowest photodegradation efficiency of 7.6 % was recorded for bare kanthal wire (0 W). This was attributed to the degradation of MB dye by UV exposure [19]. The photodegradation efficiencies increased from 17.5, 34.9, and 36.3 % with increasing heating powers from 30, 40 and 50 W, respectively. By increasing the heating power, a better surface coverage of TiO_2 particles on the kanthal wires was observed. A good surface coverage indicates that more TiO_2 particles were deposited, allowing more efficient photodegradation on MB dye. Table 5 shows a comparison of photodegradation efficiency of TiO_2 particles immobilized on various substrates with our work. Although the photodegradation efficiency was not the best as compared to other studies, it demonstrated the potential of immobilizing TiO_2 particles on kanthal wires using direct heating method.

Table 5 *A comparison of TiO_2 photodegradation efficiency immobilized on various substrates*

Substrate	Type of organic compounds	Concentration (ppm)/ Volume (ml)	Efficiency (%)	Time taken (hr)
Glass tube	Bisphenol A	10ppm	72.0	6.0
Borosilicate glass spheres	Methylene blue	10ppm	96.2	1.5
Silica gel	Dimethoate and glyphosate	17ppm & 23ppm/200ml	100.0	1.0
Polymeric substrates	Methylene blue	4ppm/100ml	~95.0	2.0
Quartz substrate	Methyl Red and Methyl Orange	8ppm & 10ppm	100.0	2.0
Kanthal coil	Methylene blue	1ppm/100ml	36.3	1.5

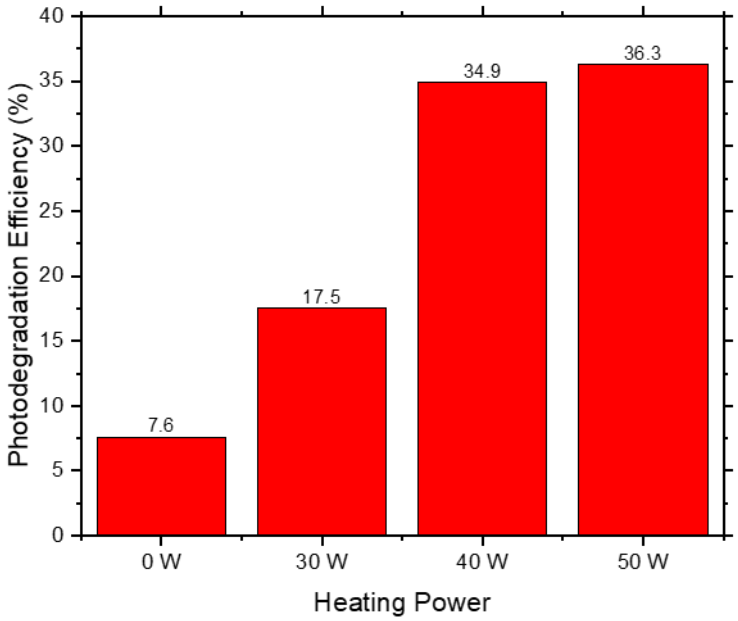

Fig. 8 *Photodegradation efficiency of MB dye degraded by TiO_2 particles produced by DH method using various heating powers under 90 min of UV light irradiation*

4. Conclusion

TiO_2 particles were successfully deposited on kanthal coils by DH method. The best heating power to deposit TiO_2 particles was 50 W. Both XRD and FTIR confirmed the existence of TiO_2. In fact, the TiO_2 particles deposited consisted of 22.5% of Anatase and 77.5% of Brookite. At this heating power, the surface coverage of TiO_2 particles on kanthal coils was good with little aggregation. The particle size is 139.34 ± 15.89 nm (n = 30). It achieved 36.3 % photodegradation efficiency on MB dye when exposed to UV light. In summary, the DH method demonstrates its potential to deposit TiO_2 particles on kanthal coils rapidly (15 min) with small electrical power usage (50 W).

Acknowledgement

This The authors gratefully acknowledge the financial support of Ministry of Higher Education, Malaysia for providing the research funding under Fundamental Research Grant Scheme (FRGS) (FRGS/1/2020/TK0/USM/02/27) to conduct this project.

Conflict of Interest

Authors declare that there is no conflict of interests regarding the publication of the paper.

Author Contribution

The authors confirm contribution to the paper as follows: ***study conception and design:*** *CM Koe, GS Ng, SY Pung;* ***data collection:*** *CM Koe, GS Ng;* ***analysis and interpretation of results:*** *CM Koe, GS Ng, SY Pung;* ***draft manuscript preparation:*** *CM Koe, GS Ng, SY Pung. All authors reviewed the results and approved the final version of the manuscript. The author confirms sole responsibility for the following: study conception and design, data collection, analysis and interpretation of results, and manuscript preparation.*

References

[1] G. Upendar, G. Biswas, K. Adhikari, & S. Dutta (2017). Adsorptive removal of methylene blue dye from simulated wastewater using shale: Experiment and modelling, *Journal of the Indian Chemical Society*, 94, 971-982. https://doi.org/10.5281/zenodo.5637047

[2] F. Sadeghfar, M. Ghaedi, & Z. Zalipour (2021), Chapter 4 - Advanced oxidation. *Interface Science and Technology*, 32, 225-324. https://doi.org/10.1016/B978-0-12-818806-4.00001-2

[3] R. Ameta, M. S. Solanki, S. Benjamin, & S. C. Ameta (2018). Chapter 6 - Photocatalysis. *Advanced Oxidation Processes for Waste Water Treatment*, 135-175. https://doi.org/10.1016/B978-0-12-810499-6.00006-1

[4] D. Ghime & P. Ghosh (2020). Advanced oxidation processes: a powerful treatment option for the removal of recalcitrant organic compounds. *Advanced Oxidation Processes-Applications, Trends, and Prospects*: IntechOpen. DOI: 10.5772/intechopen.90192

[5] A. ul Haq, M. Saeed, S. G. Khan, & M. Ibrahim(2021). Photocatalytic Applications of Titanium Dioxide (TiO 2). *Titanium Dioxide-Advances and Applications*: IntechOpen. DOI: 10.5772/intechopen.99598
[6] T.-L. T. Le, T.-H. T. Le, K. N. Van, H. Van Bui, T. G. Le, & V. Vo (2021). Controlled growth of TiO2 nanoparticles on graphene by hydrothermal method for visible-light photocatalysis. *Journal of Science: Advanced Materials and Devices,* 6, 516-527. https://doi.org/10.1016/j.jsamd.2021.07.003
[7] L.-H. Yang, T.-Y. Yang, K.-y. Wang, T.-Y. Su, D.-C. Wu, & Y.-L. Cheuh (2020). Three-dimensional CuO/TiO2 hybrid nanorod arrays prepared by electrodeposition in AAO membranes as an excellent Fenton-like photocatalyst for dye degradation. *Nanoscale research letters,* 15, 1-12. https://doi.org/10.1186/s11671-020-3266-6
[8] W. Nachit, H. A. Ahsaine, Z. Ramzi, S. Touhtouh, I. Goncharova, & K. Benkhouja (2022). Photocatalytic activity of anatase-brookite TiO2 nanoparticles synthesized by sol gel method at low temperature. *Optical Materials,* 129, 112256. https://doi.org/10.1016/j.optmat.2022.112256
[9] S.-T. Hong & L.-Y. Lin (2020). Fabrication of TiO2 nanoparticle/TiO2 microcone array photoanode for fiber-type dye-sensitized solar cells: Effect of acid concentration on morphology of microcone. *Electrochimica Acta,* 331, 135278. https://doi.org/10.1016/j.electacta.2019.135278
[10] C. Sanchez Tobon, D. Ljubas, V. Mandić, I. Panžić, G. Matijašić, & L. Ćurković (2022). Microwave-Assisted Synthesis of N/TiO2 Nanoparticles for Photocatalysis under Different Irradiation Spectra. Nanomaterials, 12, 1473. https://doi.org/10.3390/nano12091473
[11] M. Taylor, R. C. Pullar, I. P. Parkin, & C. Piccirillo (2020). Nanostructured titanium dioxide coatings prepared by aerosol assisted chemical vapour deposition (AACVD). *Journal of Photochemistry and Photobiology A: Chemistry,* 400, 112727. https://doi.org/10.1016/j.jphotochem.2020.112727
[12] K. C. Sun, M. B. Qadir, & S. H. Jeong, (2014). Hydrothermal synthesis of TiO 2 nanotubes and their application as an over-layer for dye-sensitized solar cells. *RSC advances,* 4, 23223-23230. https://doi.org/10.1039/C4RA03266G
[13] Q. Zhang & C. Li (2018). Pure anatase phase titanium dioxide films prepared by mist chemical vapor deposition. *Nanomaterials,* 8, 82. https://doi.org/10.3390/nano8100827
[14] S.-L. Chiam, Q.-Y. Soo, S.-Y. Pung, & M. Ahmadipour (2021). Polycrystalline TiO2 particles synthesized via one-step rapid heating method as electrons transfer intermediate for Rhodamine B removal. *Materials Chemistry and Physics,* 257, 123784. https://doi.org/10.1016/j.matchemphys.2020.123784
[15] S. N. Q. A. Abd Aziz, K. C. Meng, S.-Y. Pung, Z. Lockman, A. Ul-Hamid, & W. K. Tan, (2023). Rapid growth of zinc oxide nanorods on kanthal wires by direct heating method and its photocatalytic performance in pollutants removal. *Journal of Industrial and Engineering Chemistry,* 118, 226-238. https://doi.org/10.1016/j.jiec.2022.11.008
[16] G. S. Ng, C. M. Koe, & S.-Y. Pung (2023). Deposition of titanium dioxide particles on kanthal coils by direct heating technique for photodegradation of methylene blue solution. *International Journal of Nanoelectronics & Materials,* 16(1) 217-232.
[17] C. W. Huang & M. C. Wu (2020). Photocatalytic degradation of methylene blue by UV-assistant TiO2 and natural sericite composites. *Journal of Chemical Technology & Biotechnology,* 95, 2715-2722. https://doi.org/10.1002/jctb.6392
[18] T. A. Kandiel, L. Robben, A. Alkaima, & D. Bahnemann (2013). Brookite versus anatase TiO 2 photocatalysts: phase transformations and photocatalytic activities. *Photochemical & Photobiological Sciences,* 12, 602-609. https://doi.org/10.1039/c2pp25217a
[19] Sen, S., Das, C., Ghosh, N.N., Baildya, N., Bhattacharya, S., Khan, M.A., Sillanpää, M. & Biswas, G., (2022). Is degradation of dyes even possible without using photocatalysts?–a detailed comparative study. *RSC advances*, *12*(53), 34335-34345. https://doi.org/10.1039/D2RA05779D